ACS Catalysis

RESEARCH ARTICLE

pubs.acs.org/acscatalysis

Synergy between Pt and Au in Pt-on-Au Nanostructures for Chemoselective Hydrogenation Catalysis

Ke-Qiang Sun, Yong-Chun Hong, Gui-Rong Zhang, and Bo-Qing Xu*

Innovative Catalysis Program, Key Lab of Organic Optoelectronics & Molecular Engineering, Department of Chemistry, Tsinghua University, Beijing 100084, China

ABSTRACT: Supported Au nanoparticles (Au NPs) have been identified as highly selective catalysts for the chemoselective hydrogenation reaction potential for advanced and greener syntheses of many special and fine chemicals in organic chemistry, but their potential for applications has been hampered by their generally observed low activity arising from the intrinsic nobleness of gold to H_2 activation. This work deals with a synergy between Au NPs and their carrying Pt entities in Pt-on-Au nanostructures (coded as Pt_m^Au, m denoting the atomic Pt/Au ratio) for hydrocinnamaldehyde production in the chemoselective hydrogenation of cinnamaldehyde. Pt_m^Au immobilized on a noninteracting SiO_2 support (Pt_m^Au/SiO_2) showed activity 1−2 orders of magnitude higher than that of monometallic Pt/SiO_2 and Au/SiO_2 catalysts. The high activity of Pt_m^Au nanostructures also remained distinct on interacting support materials such as Al_2O_3 and carbon and when varying the reaction temperature, H_2 pressure, or both. Kinetic assessments suggest that the hydrogenation reaction could occur according to a Langmuir−Hinshelwood mechanism, in which cinnamaldehyde adsorbed on the Au surface was attacked by hydrogen atoms activated by Pt entities in the nanostructured Pt_m^Au catalysts. Pt dispersion or the size of the Pt entities and Pt−Au boundary, as well, strongly affected this synergic catalysis.

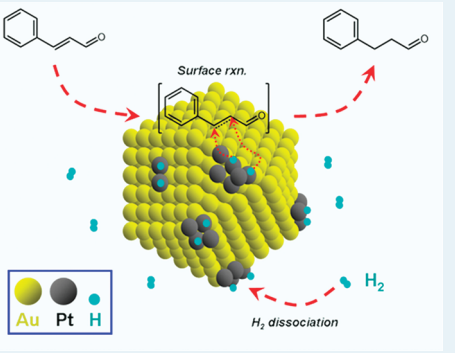

KEYWORDS: gold catalyst, Pt-on-Au nanostructure, bimetallic PtAu catalyst, selective hydrogenation, cinnamaldehyde, α,β-unsaturated aldehyde, kinetic modeling

1. INTRODUCTION

Information gained during the last couple of decades indicates that supported Au nanoparticles (Au NPs) are emerging as selective catalysts for many organic reactions, including oxidation[1−3] and hydrogenation[4−8] as well as some coupling[9,10] reactions, which are of potential for advanced and greener organic syntheses. Chemoselective hydrogenation of α,β-unsaturated aldehydes to their semihydrogenated products, that is, saturated aldehydes from hydrogenation at the C═C bond conjugated with the carbonyl group or unsaturated alcohols from hydrogenation at the C═O bond, is a critical route in the syntheses of many important chemicals, such as fragrances, pharmaceuticals, and others.[11] Supported Au NPs were found highly selective for the hydrogenation of α,β-unsaturated aldehydes, including cinnamaldehyde (CAL),[12−15] acrolein,[16,17] crotonaldehyde,[18,19] and others.[20,21] Some elegant investigations have identified that the key factors affecting the hydrogenation catalysis would include the size and morphology of Au NPs,[13,14,16−19] the nature of the supporting materials,[12−14,18] and the reaction conditions, as well.[14,21] However, the hydrogenation activity of Au was usually much lower than that of platinum-group metals,[13,18,19] which severely impairs practical application of Au catalysts.

The low activity of Au for hydrogenation reactions was generally attributed to an "intrinsic" nobleness of Au for H_2 activation. The dissociative adsorption of H_2 on Au is an activated process, which would be restricted only at the edge and corner sites[22,23] or perimeter interfaces of Au NPs in close contact with an oxide support.[24] This H_2 activation step was believed to be the rate-limiting step in several hydrogenation reactions, such as gas phase hydrogenation of butadiene[25] and liquid phase hydrogenation of nitrobenzene.[8] The chemisorption of H_2 on Au NPs was found very sensitive to the presence of a more active metal (e.g., Pt).[23,26] In this light, Corma et al. showed that the activity of Au/TiO_2 for chemoselective hydrogenation of nitrostyrene was enhanced remarkably after it was impregnated with a small amount of Pt.[8]

We showed earlier that Au NPs immobilized on SiO_2 (Au/SiO_2) were highly selective for the formation of hydrocinnamaldehyde (HCAL) in the hydrogenation of CAL.[14] We also communicated[15] very recently that the activity of Au NPs (3.0 nm) in the hydrogenation of α,β-unsaturated carbonyl compounds, including CAL, furfural, and chalcones, can be dramatically improved (up to 70-fold) when a very small amount of fully dispersed Pt entities was properly loaded at the surface of Au NPs to form Pt-on-Au nanostructures (coded as Pt_m^Au, m denoting the atomic Pt/Au ratio[27−30]). It was proposed that the Pt entities in these catalytic nanostructures were serving as the activity promoter of Au NPs, since the selectivity propensity of Au NPs for the hydrogenation reactions was not changed by the presence of Pt.

This work presents a systematic investigation on the characteristics of immobilized Pt_m^Au nanostructures in hydrogenation

Received: May 13, 2011
Revised: July 18, 2011
Published: August 29, 2011

catalysis using CAL hydrogenation as a probe reaction. Pt_m^Au NPs of varying compositions ($0 \le m \le 0.2$) are immobilized onto three different supporting materials (that is, noninteracting SiO_2 and interacting Al_2O_3 and carbon) to understand any possible support effect. The influences of reaction temperature and hydrogen pressure on the hydrogenation catalysis of these immobilized Pt_m^Au catalysts are also disclosed. Kinetic analysis of the hydrogenation reaction is conducted to gain information on the catalytic mechanism and synergy between Pt and Au in the catalytic Pt_m^Au nanostructures.

2. EXPERIMENTAL METHODS

2.1. Preparation of Au and Pt_m^Au NPs. Au NPs were prepared as PVA-stabilized colloidal particles (3.0 ± 0.6 nm) by reduction of $AuCl_4^-$ ions in aqueous solution containing $HAuCl_4$ (99%, Acros) and poly(vinyl alcohol) (PVA, CP, Beijing Chemical Reagent Company, typical repeating units 1750) with $NaBH_4$ (98%, Sigma-Aldrich), as described elsewhere.[2,14,15,28−30] In a typical procedure, 200 mL of 0.25 mM $HAuCl_4$ solution was mixed with 1 mL of PVA solution (10 mg mL^{-1}). The solution was stirred for 1 h, and then 5 mL of fresh 0.1 M $NaBH_4$ solution was added dropwise under vigorous stirring. The resulting wine-colored solution was kept under stirring for 2 h to ensure complete $AuCl_4^-$ reduction to form Au NPs. The produced Au NPs showed a narrow size distribution at 3.0 ± 0.6 nm, and were used later to prepare Pt_m^Au nanostructures.

Pt_m^Au NPs ($0.005 \le m \le 0.2$) were synthesized by reductive deposition of Pt onto the preformed PVA-stabilized Au NPs, as previously described.[15,28−30] In the preparation of $Pt_{0.05}$^Au NPs, for example, 50 mL of 0.05 mM K_2PtCl_6 (AR, Beijing Chemical Reagent Company) solution (2.5 μmol Pt) was mixed with the as-prepared colloidal Au solution (ca. 50 μmol Au). The mixed solution was stirred for 2 h and then purged with N_2 for 30 min, followed by bubbling with H_2 for another 2 h. A gradual Pt deposition on the Au NPs was evidenced by the solution color change from wine red to dark brown. When the H_2 bubbling was stopped, the colloidal solution was sealed airtight and was then allowed to remain undisturbed for 48 h to ensure complete Pt deposition. Element analysis (ICP-AES) showed that Pt deposition during these syntheses was 100% quantitative.

2.2. Immobilization of Au and Pt_m^Au NPs and Postsynthesis Treatment. Three support materials—SiO_2 (90 m^2 g^{-1}, Degussa Aerosil 90), Al_2O_3 (160 m^2 g^{-1}) prepared from hydrolysis of $Al(NO_3)_3$ with aqueous ammonia solution,[31] and carbon black (250 m^2 g^{-1}, Vulcan XC-72)—were employed to immobilize Au and Pt_m^Au NPs. It should be noted that the Au NPs were also subjected before the immobilization process to a H_2 bubbling treatment but without the addition of K_2PtCl_6.

Immobilization of Au or Pt_m^Au NPs with SiO_2 and Al_2O_3 supports was conducted using procedures reported previously.[2,14,15] In brief, desirable amounts of the support materials were added into colloidal solutions containing Au or Pt_m^Au NPs, followed by careful adjustment of the solution acidity (pH = 0.5 in the case of SiO_2, pH = 6.0 in the case of Al_2O_3) with aqueous solution of HNO_3 under vigorous stirring. HNO_3 solution of different concentrations (0.2, 1.0, and 3.2 M) was alternatively used to avoid any rapid drop in the pH. The solids were then separated by filtration, followed by extensive washing with deionized water and drying at 110 °C; the actual Au loadings in these samples were ~1.0 wt % by ICP-AES analysis.

The immobilization of Au or Pt_m^Au NPs with carbon (XC-72) was conducted following the procedure detailed previously.[27−30] Briefly, a desirable amount of Vulcan XC-72 carbon black was added to a colloidal solution containing Au or Pt_m^Au NPs. After adjustment of the solution acidity (pH = 1.5) with an aqueous solution of HNO_3, the mixed solution was refluxed for 2 h under vigorous stirring. The solids were then separated by filtration, followed by extensively washing with deionized water and drying at 110 °C to produce Au/XC-72 or Pt_m^Au/XC-72 catalyst; the actual Au loadings on the carbon support were ~5.0 wt % by ICP-AES analysis.

2.3. Preparation of Bimetallic Pt−Au/SiO_2 Catalyst. A bimetallic Pt−Au/SiO_2 sample was also prepared for comparison purposes by impregnating Pt on our standard Au/SiO_2 sample according to the procedure of Corma et al.[8] Briefly, 1.0 g of Au/SiO_2 sample prepared as above was added to 50 mL of 0.05 mM K_2PtCl_6 solution. After stirring at room temperature for 24 h, the suspension liquids were evaporated at 60 °C using a rotary evaporator. The solids obtained as such were dried at 110 °C. This reference sample was denoted as $Pt_{0.05}$-Au/SiO_2, as the atomic Pt/Au ratio was 0.05 according to the ICP-AES analysis.

Two reference SiO_2-supported Pt catalysts with Pt loading of 1 wt % (1Pt/SiO_2−Sigma; BET surface area: 275 m^2/g) and 5 wt % Pt (5Pt/SiO_2−Strem; BET surface area: 400 m^2/g) were purchased from Sigma-Aldrich (Lot no: 07204HU) and Strem (Lot no: 18091300), respectively. The Pt dispersions in these two samples were lower than 0.30. Another Pt/SiO_2 sample with fully dispersed Pt was prepared according the method of Miller et al.[32]

2.4. Characterizations. The actual loadings of Au and Pt in each of the as-prepared samples were determined by ICP-AES analysis (Leeman2000 Prodigy spectrometer). The morphology and size distribution of Au and Pt_m^Au NPs before and after immobilization were characterized by transmission electron microscopy (TEM) using a Tecnai G2 F20 U-Twin system operating at 200 kV. At least 300 particles were randomly measured to determine the mean diameter of Au and Pt_m^Au NPs according to the equation $d = \sum n_i d_i / \sum n_i$, where n_i and d_i are the number and diameter of the NPs, respectively.

The dispersions of Pt (D_{Pt}) in Pt_m^Au NPs were determined by cyclic voltammetry (CV) measurement of immobilized Pt_m^Au NPs on XC-72. The cyclic voltammetry was conducted in 0.5 M H_2SO_4 at a scan rate of 20 mV s^{-1}. Given the well-established hydrogen-adsorption stoichiometry at a Pt surface (H/Pt = 1:1), the number of the exposed Pt atoms (N_s) was counted as the number of adsorbed hydrogen atoms (N_H) by integrating the charge consumed for hydrogen desorption (Q_H) on the CV curve, that is $N_s = N_H = Q_H/Q_e$, where Q_e is the elementary charge or charge of an electron (1.602×10^{-19} C). Thus, the ratio of N_s to the total number of Pt atoms (N_t) in the catalyst gives the dispersion of Pt: $D_{Pt} = N_s/N_t$. Further details for these measurements were given in refs 27−30.

The dispersion of Pt (D_{Pt}) in the reference Pt/SiO_2 catalysts was determined by H_2-TPD measurement, which was conducted on homemade equipment as described previously.[33] The sample was first reduced at 300 °C in 5 vol % H_2−Ar flow for 1 h and then held at 150 °C for 1 h before cooling to room temperature in the same gas flow. The gas flow was then switched to a flow of ultrahigh purity Ar (99.999%), which was further online purified by flowing through two traps containing 5A zeolite and MnO_x-based deoxidant, respectively. The temperature ramp was 10 °C/min. The number of exposed Pt atoms in the sample was counted as the number of H atoms in the desorbed H_2 molecules measured from the H_2-TPD experiment.

dx.doi.org/10.1021/cs200247r |ACS Catal. 2011, 1, 1336–1346

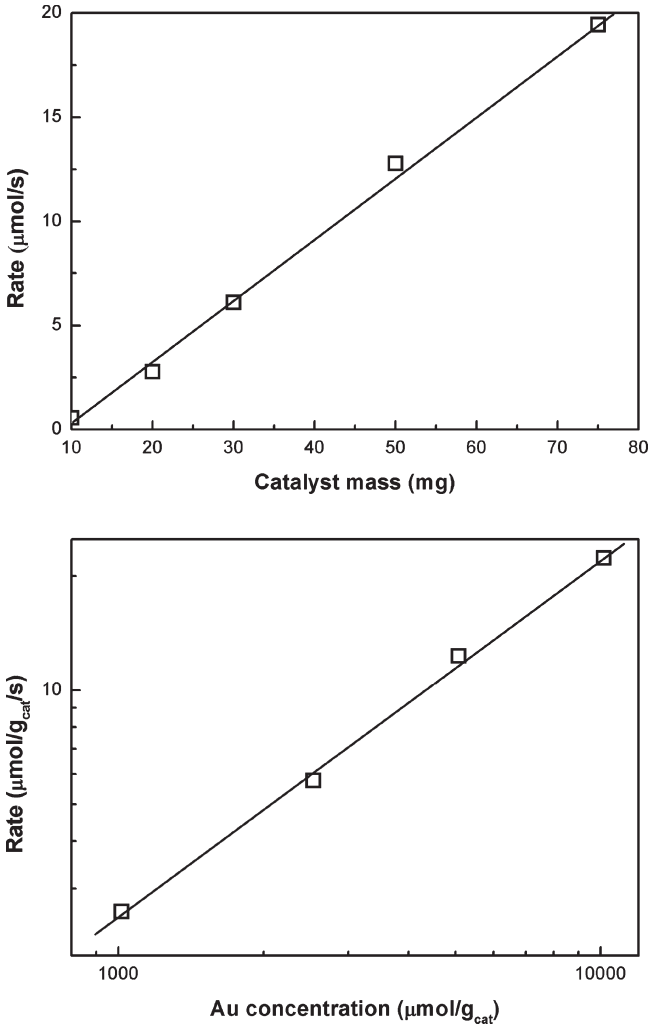

Figure 1. Effect of catalyst mass (A) and $Pt_{0.05}$^Au loading (B: the Madon-Boudart test) on the reaction rate of cinnamaldehyde hydrogenation using the $Pt_{0.05}$^Au/SiO_2 catalyst. Reaction temp = 150 °C; P_{H_2} = 1.0 MPa; 4 mmol of CAL in 5 mL of toluene; stirring speed = 900 rpm.

2.5. Catalytic Test and Product Analysis. Hydrogenation reactions were performed on a high-pressure batch reactor equipped with a Parr 4843 controller and a 25 mL Hastelloy autoclave. Unless otherwise specified, the autoclave was loaded with 5 mL of toluene (AR, Beijing Chemical Reagent Company), 0.5 mL of CAL (AR, Sigma-Aldrich), and 50 mg of catalyst (molar CAL/Au = 1600). After purging with H_2 (~0.8 MPa) six times, the autoclave was pressurized to a desired H_2 pressure (e.g., 1.0 MPa) at room temperature. Zero reaction time was taken as soon as the autoclave was heated to the reaction temperature (e.g., 150 °C), and the mechanical stirring (900 rpm) was not switched on until that very moment. Preliminary experiments performed using varying stirring speeds (in the range of 500−1200 rpm) showed that the selected stirring speed (900 rpm) enabled the reaction to proceed in the absence of diffusion limitation under the present reaction conditions. The absence of mass transfer effect on the reaction rate in our system was also double-checked by changing the catalyst mass (10−75 mg) for the reaction and applying the Madon−Boudart test[34] using $Pt_{0.05}$^Au/SiO_2 catalyst of varied metal loadings, as shown in Figure 1.

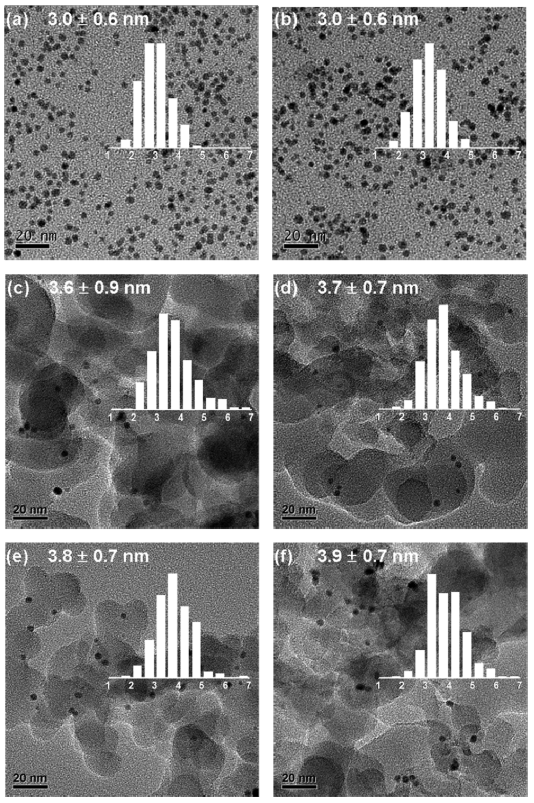

Figure 2. Representative TEM images: (a) colloidal Au NPs, (b) colloidal $Pt_{0.05}$^Au NPs, (c) Au/SiO_2, (d) $Pt_{0.01}$^Au/SiO_2, (e) $Pt_{0.05}$^Au/SiO_2, and (f) $Pt_{0.1}$^Au/SiO_2. The accompanying bar graphs give the size distributions of the Au or Pt_m^Au NPs.

An ice−water bath was used to cool the autoclave at the end of each reaction. The reacted liquid was separated from catalyst powders by filtration and then analyzed by a HP-7890A gas chromatograph (GC) equipped with a Shimadzu HiCap CBP20 capillary column and a flame ionization detector. Product identification was double-checked, when necessary, with a HP-6890 GC equipped with a HP-5973 mass selective detector.

3. RESULTS

3.1. Characterization of Pt_m^Au Nanostructures. Shown in Figure 2 are representative TEM images of colloidal and immobilized Au and Pt_m^Au NPs. The colloidal Au NPs were nearly monodispersed and spherically shaped with sizes in the range 3.0 ± 0.6 nm (Figure 2a). The Pt_m^Au NPs showed similar sizes and size distributions (Figure 2a, b).[28,30] Some representative TEM images for the silica immobilized Au (Au/SiO_2) and Pt_m^Au NPs (Pt_m^Au/SiO_2) samples are shown as Figure 2c−f. Compared with their unimmobilized counterparts in colloidal solutions, the immobilized Au and $Pt_{0.05}$^Au NPs showed slightly larger sizes, but their size distributions still remained quite narrow. The TEM images of metal particles for Pt_m^Au/Al_2O_3 and Pt_m^Au/XC-72 samples of m = 0 and 0.05 (data not shown) were found very similar to those of Pt_m^Au/SiO_2 with the same composition, suggesting that the features of these Pt_m^Au NPs were not changed during the immobilization process.[15,28−30] The sizes of Pt_m^Au NPs in Pt_m^Au/SiO_2 became a little larger with the increase in m (Figure 2d−f) due to increased covering of Pt at the Au surfaces.

dx.doi.org/10.1021/cs200247r |ACS Catal. 2011, 1, 1336–1346

Quantitative measurement of Pt dispersion in Pt_m^Au NPs was done via an electrochemical approach; namely, CV in acidic solution of the Pt_m^Au/XC-72 samples.[27−30] Figure 3 shows some typical CV curves for several Pt_m^Au/XC-72 samples ($0 \le m \le 0.2$) recorded at room temperature in N_2-purged 0.5 M H_2SO_4 solution. The signals in the potential region of −0.2 to 0.14 V (relative to a saturated calomel electrode) are distinctive of hydrogen adsorption/desorption chemistry associated only with the Pt entities in the samples (Au NPs were inert for this chemistry; see the insert in Figure 3 and also refs 28−30). The charge associated with the hydrogen desorption peaks (i.e., positive peaks on the CV curves) was used to obtain Pt dispersion data (D_{Pt}),[27−30] which are listed in the second column of Table 1. The Pt entities were found fully dispersed ($D_{Pt} \approx 0.99$) in the Pt_m^Au samples at $m \le 0.05$. In other words, every Pt atom in these samples was exposed and could be available for surface catalysis.[15,27,28] The Pt dispersion decreased to 0.90 and 0.62, respectively, when m was increased to 0.1 and 0.2. The hydrogen desorption peak shifted toward lower potential for Pt_m^Au/XC-72 with the decrease in m, which could give a hint of the dispersive structure of Pt entities in $Pt_{0.01}$^Au and $Pt_{0.005}$^Au NPs.[28] These results in combination with previous comprehensive characterizations (UV−vis, SERS, XPS, and XRD)[27−30] would suggest that Pt entities exist as highly dispersed ($D_{Pt} \ge 0.60$) cluster islands or two-dimensional rafts at the surfaces of Au NPs in the Pt_m^Au samples ($m \le 0.2$).

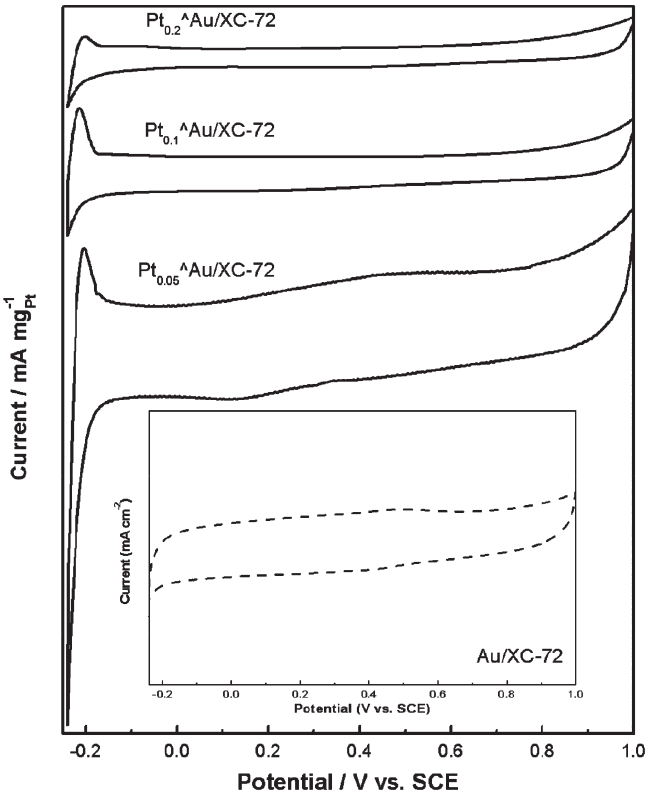

Figure 3. Cyclic voltammetry curves of Pt_m^Au/XC-72 samples recorded at 25 °C in N_2-purged 0.5 M H_2SO_4 (scan rate = 20 mV s^{-1}). The inset shows the CV curve of Au/XC-72 sample recorded at the same condition.

3.2. Chemoselective Hydrogenation of CAL. Shown in Scheme 1 are the reactions that could be involved in the hydrogenation of CAL. Hydrogenation at the C═C bond produces hydrocinnamaldehyde (HCAL), an important intermediate for the syntheses of pharmaceuticals for the treatment of AIDS,[35] whereas hydrogenation at the C═O bond produces cinnamyl alcohol (COL), a pharmaceutical intermediate for syntheses of cinnarizine, naftifine, toremifene, etc. Further hydrogenation of these two semihydrogenated products would lead to hydrocinnamyl alcohol (HCOL). To avoid a potential transfer hydrogenation of CAL with hydrogen-releasing solvent (for example, benzyl alcohol[15]), toluene was employed as the solvent because it was inert during the hydrogenation reaction.[14,15]

Table 1. Catalytic Results of Cinnamaldehyde Hydrogenation.[a]

				selectivity (%)				
catalyst	D_{Pt}	reaction time (min)	CAL conversion (%)	HCAL	COL	HCOL	MSA_{Au}[b]	TOF_{Pt}[c]
SiO_2		720	0					
Au/SiO_2[d]		720	11	73	23	4	0.07 (1)[e]	
$Pt_{0.005}$^Au/SiO_2[d]	0.99	240	20	77	15	8	0.40 (6)	4.42
$Pt_{0.01}$^Au/SiO_2[d]	0.99	120	19	79	17	4	0.76 (11)	4.42
$Pt_{0.05}$^Au/SiO_2[d]	0.99	15	15	72	19	9	4.77 (68)	5.24
$Pt_{0.05}$^Au/SiO_2[f]	0.99	120	87	75	21	4		
$Pt_{0.1}$^Au/SiO_2[d]	0.90	15	16	71	21	8	5.09 (73)	3.11
$Pt_{0.2}$^Au/SiO_2[d]	0.62	15	15	75	19	6	4.77 (68)	2.12
$Pt_{0.05}$-Au/SiO_2		90	20	75	20	5	1.02 (15)	
$1Pt/SiO_2$−NH_3	0.99	120	15	79	12	9		0.03
$1Pt/SiO_2$−Sigma	0.16	120	18	53	40	7		0.24
$5Pt/SiO_2$−Strem[d]	0.25	120	14	84	13	4		0.13
Au/Al_2O_3		120	5	65	28	7	0.19 (3)	
$Pt_{0.05}$^Au/Al_2O_3	0.99	15	11	76	18	6	3.36 (48)	3.84
Au/XC-72		240	15	63	32	5	0.28 (4)	
$Pt_{0.05}$^Au/XC-72	0.99	10	8	72	22	6	3.82 (55)	4.20

[a] Reaction temp = 150 °C; P_{H_2} = 1.0 MPa; CAL = 4 mmol; stirring speed = 900 rpm. [b] Mass-specific activity of Au, mol h^{-1} g_{Au}^{-1}. [c] Obtained by assuming that the exposed Pt atoms were solely responsible for the activity, s^{-1}. [d] The data in these lines were also reported in ref 15. [e] Data in the parentheses give the numbers relative to the Au/SiO_2 catalyst. [f] Data in this line were obtained with a reaction temperature of 180 °C.

dx.doi.org/10.1021/cs200247r |ACS Catal. 2011, 1, 1336–1346

Scheme 1. Reactions Involved in the Hydrogenation of Cinnamaldehyde

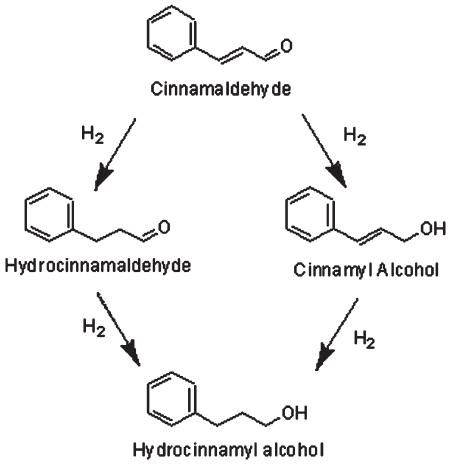

3.2.1. Effect of Pt Entities in Pt_m^Au/SiO_2. Figure 4 presents the effect of Pt in Pt_m^Au/SiO_2 on the catalytic hydrogenation of CAL. Au/SiO_2 catalyst with no Pt (m = 0) showed a strong propensity toward the formation of HCAL (73% selectivity) but produced a low CAL conversion (~4%) in a reaction period of 4 h under the standard reaction condition (150 °C, P_{H_2} = 1.0 MPa). The deposition of a very small amount of Pt (m = 0.005, Pt loading = ~0.005 wt %) on the Au NPs elevated the CAL conversion to 20%, a 5-fold increment in the same duration of reaction (4 h). Increasing m to 0.01 and 0.05 resulted in increments of the CAL conversion to 38% and 65%, respectively. However, the conversion of CAL was not enhanced on further increasing the Pt amount to m = 0.1 (66%) and even decreased to 47% at m = 0.2. It should be noted that the hydrogenation selectivity to HCAL over these Pt_m^Au/SiO_2 catalysts basically remained unchanged (75−80%, Figure 4).

For a rigorous comparison of the catalytic activity of Au in these Pt_m^Au/SiO_2 catalysts, the CAL conversion level was restrained in the range of 11−20% by adjusting the duration of the catalytic reaction (Table 1). The CAL conversion data were then used to calculate the reaction rates by CAL consumption according to the mass of gold (MSA_{Au}, mass specific activity of Au, in mol h^{-1} g_{Au}^{-1}) and the number of exposed metal atoms (TOF, turnover frequency, s^{-1}). The MSA_{Au} numbers are listed in the second to last column of Table 1. The MSA_{Au} for Au/SiO_2 (m = 0) was as low as 0.07 mol h^{-1} g_{Au}^{-1} and was enhanced to 6-, 11-, 68-, 73- and 68-fold higher for Pt_m^Au/SiO_2 of m = 0.005, 0.01, 0.05, 0.1 and 0.2, respectively. It is of interest to note that the catalysts of m = 0.05, 0.1, and 0.2 showed very close MSA_{Au} numbers (4.8−5.1 mol h^{-1} g_{Au}^{-1}). In contrast to the dramatic activity change, the product selectivity was found not affected by the deposition of Pt entities. The product distribution of CAL hydrogenation over Au/SiO_2 and Pt_m^Au/SiO_2 (columns 5−7 in Table 1) was very close: the selectivity to HCAL was in the range of 71−79%, and that to COL, 15−23%. It should be noted that this kind of product distribution was not changed when the conversion of CAL was increased up to 87% over the $Pt_{0.05}$^Au/SiO_2 (see Table 1).

An obviously different product distribution was observed over the two Pt/SiO_2 catalysts, 1Pt/SiO_2−Sigma (D_{Pt} = 0.16) and 5Pt/SiO_2−Strem (D_{Pt} = 0.25) (Table 1), which could be related to the effect of Pt dispersion.[36] The product selectivity over the former catalyst (HCAL selectivity of 53%, COL selectivity of 40%) was quite different but that over the latter catalyst (HCAL selectivity of 84%, and COL selectivity of 13%) resembled those over the Pt_m^Au/SiO_2 catalysts. To ascertain the effect of Pt dispersion in Pt/SiO_2 on the reaction selectivity, we prepared according to the report of Miller et al.[32] another Pt/SiO_2 catalyst (i.e., 1Pt/SiO_2−NH_3) that contained fully dispersed Pt (D_{Pt} ≈ 99). The product distribution over this 1Pt/SiO_2−NH_3 catalyst also demonstrates a high selectivity for HCAL (79%) over fully dispersed metallic Pt catalyst. Thus, the selectivity characteristics of Pt_m^Au/SiO_2 catalysts are more similar to those of Au/SiO_2 and Pt/SiO_2 featuring highly dispersed Pt, rather than those of Pt/SiO_2 with poorly dispersed Pt.[36] These results indicate that the deposition of a small amount of highly dispersed Pt on the Au surface dramatically enhanced the Au activity for CAL hydrogenation without altering the selectivity propensity of Au NPs.

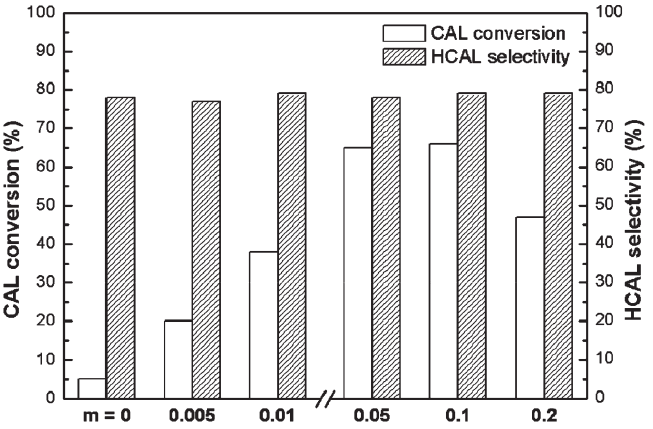

Figure 4. Influence of the atomic Pt/Au ratio (m) on cinnamaldehyde conversion and hydrocinnamaldehyde selectivity in the hydrogenation of cinnamaldehyde over Pt_m^Au/SiO_2 catalysts. Reaction temp = 150 °C; P_{H_2} = 1.0 MPa; CAL/Au = 1600 (molar); stirring speed = 900 rpm; reaction time = 4 h.

The numbers in the last column of Table 1 show the turnover frequency of CAL based on exposed Pt (TOF_{Pt}), assuming that the exposed Pt atoms were the catalytic sites responsible for the observed activity. Compared with the data for the reference Pt/SiO_2 catalysts (0.03−0.24 s^{-1}), the TOF_{Pt} for every Pt_m^Au/SiO_2 catalyst was 1−2 orders of magnitude higher (2.1−5.2 s^{-1}). In addition, it is worth noting that among the Pt_m^Au/SiO_2 catalysts, the fully dispersed Pt (D_{Pt} ≈ 0.99 at m ≤ 0.05) showed very similar TOF_{Pt} numbers (4.4−5.2 s^{-1}) that were significantly higher than those for the samples with less dispersed Pt (Pt_m^Au/SiO_2 at m ≥ 0.1). The surprisingly low TOF_{Pt} of the Pt/SiO_2 catalysts, though increased with a decrease in the Pt dispersion (0.03 s^{-1} at D_{Pt} = 0.99 and 0.24 s^{-1} at D_{Pt} = 0.16), would suggest a synergic effect between the Pt entities and the Au NPs in the Pt_m^Au/SiO_2 catalysts, which will be addressed in the discussion later.

A recent study on chemoselective hydrogenation of nitrostyrene by Corma et al. found that the catalytic activity of 1.5%Au/TiO_2 catalyst (World Gold Council) was remarkably improved after it was loaded by impregnation with very small amounts of Pt.[8] The activity based on exposed Au atoms (or mass of Au if the sizes of Au NPs were not changed) was improved by 8 times at a loading of 0.01% Pt (Pt/Au = 0.007, denoted as 1.5%Au@0.01% Pt/TiO_2 in ref 8), without scarifying the chemoselectivity for vinylaniline (>90%) of the original 1.5%Au/TiO_2 catalyst.

dx.doi.org/10.1021/cs200247r |ACS Catal. 2011, 1, 1336–1346

Table 2. Effect of Reaction Temperature on the Hydrogenation of Cinnamaldehyde over Au/SiO_2 and $Pt_{0.05}$^Au/SiO_2.[a]

catalyst	reaction temp. (°C)	reaction time (min)	CAL conversion (%)	selectivity (%)			rate[b]
				HCAL	COL	HCOL	
Au/SiO_2	150	720	11	73	23	4	0.7
Au/SiO_2	165	540	15	62	33	5	1.3
Au/SiO_2	180	160	17	63	32	5	2.3
Au/SiO_2	195	180	14	55	40	6	3.7
$Pt_{0.05}$^Au/SiO_2	135	60	7	73	13	14	13.2
$Pt_{0.05}$^Au/SiO_2	150	30	6	78	13	9	22.0
$Pt_{0.05}$^Au/SiO_2	165	15	5	75	15	10	36.0
$Pt_{0.05}$^Au/SiO_2	180	10	6	75	19	6	67.3

[a] P_{H_2} = 1.0 MPa; CAL = 4 mmol; stirring speed = 900 rpm. [b] CAL consumption rate, mmol h^{-1} g_{cat}^{-1}, normalized to the amount of catalyst (50.0 mg for Au/SiO_2 and 20.0 mg for $Pt_{0.05}$^Au/SiO_2).

In the present work, a bimetallic $Pt_{0.05}$—Au/SiO_2 catalyst (Pt/Au = 0.05) was prepared according to the method of Corma et al.;[8] that is, by impregnation of Pt onto our standard Au/SiO_2 catalyst. We would anticipate that most Pt in this $Pt_{0.05}$—Au/SiO_2 sample would land directly on the surface of the SiO_2 support, since the immobilized Au NPs in the standard Au/SiO_2 could occupy only a small part of the SiO_2 surface (less than 1%). The catalytic CAL hydrogenation data over this $Pt_{0.05}$—Au/SiO_2 catalyst are compared in Table 1 with those of Pt_m^Au/SiO_2 catalysts. Although the chemoselectivity property of $Pt_{0.05}$—Au/SiO_2 (75% of HCAL and 20% of COL) varied little from those of Pt_m^Au/SiO_2 (Table 1), the MSA_{Au} for $Pt_{0.05}$—Au/SiO_2 was improved only up to 15-fold of the standard Au/SiO_2 catalyst. This 15-fold activity enhancement is far inferior to the 68-fold improvement obtained over $Pt_{0.05}$^Au/SiO_2, suggesting that the Pt-on-Au nanostructure is more efficient than the bimetallic $Pt_{0.05}$—Au/SiO_2 catalyst in promoting the hydrogenation catalysis.

In the study of Corma et al.,[8] the bimetallic Pt—Au/TiO_2 catalysts preserved the chemoselectivity of the Au catalyst only at very low Pt loadings (Pt/Au ≤ 0.007). Significant decline in the chemoselectivity was observed when the Pt loading in Pt—Au/TiO_2 was increased to higher than 0.05 wt % (Pt/Au > 0.033). For instance, the selectivity for vinylaniline was lowered from 90+% over 1.5% Au/TiO_2 and 0.01% Pt—1.5% Au/TiO_2 to less than 40% over 0.2% Pt—1.5% Au/TiO_2 (Pt/Au = 0.13, denoted as 1.5%Au@0.2%Pt/TiO_2 in ref 8), such a low chemoselectivity actually signified the characteristics of Pt/TiO_2 catalyst.[8] In contrast, the present Pt_m^Au/SiO_2 catalysts can maintain the chemoselectivity of Au NPs for CAL hydrogenation even when the Pt loading was as high as 0.2 wt % (m = 0.2)

3.2.2. Effect of Support Material. The nature of the support material would remarkably affect the performance of the Au catalyst.[12−14,18] The interacting supports such as Al_2O_3 and carbon (XC-72) were used as alternatives to the noninteracting SiO_2 support to immobilize Au and $Pt_{0.05}$^Au NPs. The Au/Al_2O_3 and Au/XC-72 catalysts were found significantly more active than Au/SiO_2 for CAL hydrogenation, as the MSA_{Au} numbers for the former two catalysts were 3−4 times higher than that of Au/SiO_2 (Table 1). The enhanced activity of Au NPs in these Au/Al_2O_3 and Au/XC-72 catalysts could be ascribed to a promoted H_2 activation at the interfaces between the interacting support and Au NPs[24] or by the function of surface hydroxyl groups on Al_2O_3 and carbon materials.[25,37] The $Pt_{0.05}$^Au/Al_2O_3 and $Pt_{0.05}$^Au/XC-72 catalysts also showed dramatically higher activity than their counterparts without Pt: the MSA_{Au} for $Pt_{0.05}$^Au/Al_2O_3 was 16-fold higher than that for Au/Al_2O_3, whereas a 14-fold enhancement in MSA_{Au} was registered for $Pt_{0.05}$^Au/XC-72 than that for Au/XC-72 (Table 1), indicating that the promotion effect of Pt on the catalytic activity of Au NPs also prevails on the interacting supports.

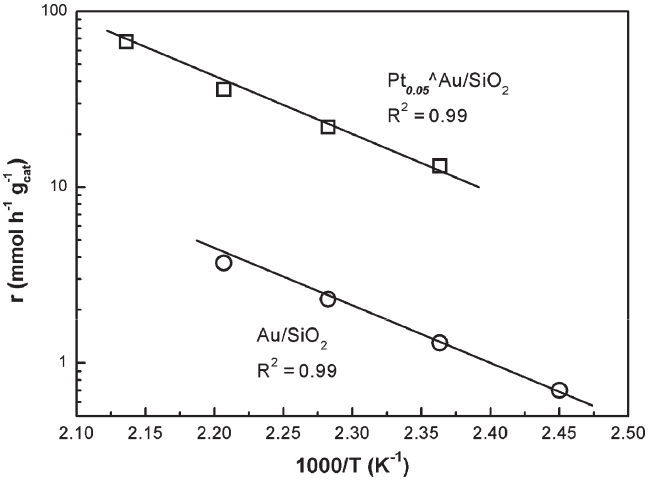

Figure 5. Arrhenius plots for the cinnamaldehyde hydrogenation over Au/SiO_2 and $Pt_{0.05}$^Au/SiO_2 catalysts.

On the other hand, the interacting supports strongly affected the product selectivity of the Au NPs.[12−14,18] In the present study, changing the support from the noninteracting SiO_2 to the interacting Al_2O_3 and carbon increased the selectivity for COL production from ∼20 to ∼30% at the expense of losing the selectivity for HCAL production. However, the selectivity for the fully hydrogenated product HCOL was little affected by the nature of the support materials. Lewis acid sites at the surface of Al_2O_3 would favor the adsorption of CAL with the carbonyl group, which could be responsible for the increased selectivity for COL.[38] The supporting carbon material could act as an electron-donating macroligand, which would lead to electron-rich Au NPs and enable the higher selectivity for COL.[39] Interestingly, the product distribution obtained with the $Pt_{0.05}$^Au/Al_2O_3 and $Pt_{0.05}$^Au/XC-72 catalysts deviated significantly from those with the Au/Al_2O_3 and Au/XC-72 and instead resembled those with the Au/SiO_2 and Pt_m^Au/SiO_2

dx.doi.org/10.1021/cs200247r |ACS Catal. 2011, 1, 1336–1346

Table 3. Effect of H_2 Pressure on the Hydrogenation of Cinnamaldehyde over Au/SiO_2 and $Pt_{0.05}$^Au/SiO_2.[a]

catalyst	P_{H_2} (MPa)	reaction time (min)	CAL conversion (%)	selectivity (%) HCAL	COL	HCOL	rate[b]
Au/SiO_2	1.0	720	11	73	23	4	0.7
Au/SiO_2	2.0	240	13	62	33	5	2.6
Au/SiO_2	3.0	120	10	49	44	7	4.1
Au/SiO_2	4.0	60	10	51	44	5	7.8
Au/SiO_2	5.0	30	7	53	39	8	10.7
$Pt_{0.05}$^Au/SiO_2	0.5	60	4	78	12	10	8.6
$Pt_{0.05}$^Au/SiO_2	1.0	30	6	78	13	9	22.0
$Pt_{0.05}$^Au/SiO_2	2.0	15	6	76	16	8	47.2
$Pt_{0.05}$^Au/SiO_2	3.0	10	8	74	16	10	102.0
$Pt_{0.05}$^Au/SiO_2	4.0	10	10	72	18	10	118.8

[a] Reaction temp = 150 °C; CAL = 4 mmol; stirring speed = 900 rpm. [b] CAL consumption rate, mmol h^{-1} g_{cat}^{-1}, normalized to the amount of catalyst (50.0 mg for Au/SiO_2 and 20.0 mg for $Pt_{0.05}$^Au/SiO_2).

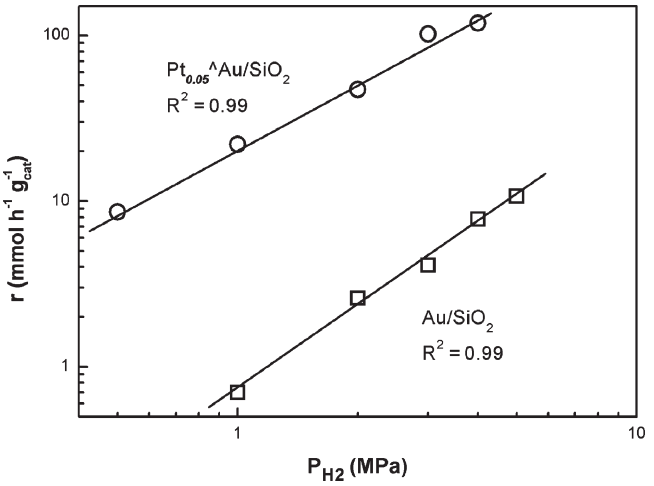

Figure 6. Effect of H_2 pressure on the overall rate of cinnamaldehyde hydrogenation over Au/SiO_2 and $Pt_{0.05}$^Au/SiO_2 catalysts.

catalysts (Table 1). These results clearly indicate that the catalysis of Pt_m^Au NPs is insensitive to the nature of the support materials, although the catalysis of its counterpart Au NPs was sensitive to metal−support interaction.

3.2.3. Effects of Reaction Temperature and H_2 Pressure. It is known that the chemoselectivity in hydrogenation of α,β-unsaturated aldehydes depends significantly on the reaction temperature and H_2 pressure.[14,21] Au and $Pt_{0.05}$^Au NPs immobilized on the noninteracting support SiO_2 were then used to show the effects of reaction temperature and H_2 pressure (P_{H_2}) on the hydrogenation of CAL. To reduce the deviation in measuring the catalytic rates, CAL conversion levels in these experiments were also limited to <20% by adjusting the duration of the reaction (Au/SiO_2) and the amount of catalyst when necessary ($Pt_{0.05}$^Au/SiO_2). Table 2 shows the catalytic results. The data in the last column give the global reaction rates by CAL consumption normalized to the catalyst mass (mmol h^{-1} g_{cat}^{-1}). Increasing the reaction temperature from 150 to 195 °C for Au/SiO_2 and from 135 to 180 °C for $Pt_{0.05}$^Au/SiO_2 resulted in continuous shortening of the reaction period for achieving a certain CAL conversion (~15% for Au/SiO_2 and ~5% for $Pt_{0.05}$^Au/SiO_2). The reaction rate increased 5-fold for both Au/SiO_2 and $Pt_{0.05}$^Au/SiO_2 catalysts when the reaction temperature was elevated by 45 °C. The nearly parallel Arrhenius plots derived from the reaction rates over Au/SiO_2 and $Pt_{0.05}$^Au/SiO_2 catalysts are shown in Figure 5. The corresponding apparent activation energy (E_a) and pre-exponential factor (A) were 59 kJ mol^{-1} and 4.1 mmol h^{-1} g_{cat}^{-1} for Au/SiO_2 and 55 kJ mol^{-1} and 40.0 mmol h^{-1} g_{cat}^{-1} for $Pt_{0.05}$^Au/SiO_2 catalyst (Table 4). These E_a numbers are lower than the activation energy (E_a = ~65 kJ mol^{-1}) of CAL hydrogenation over Pd/C catalyst in toluene solvent.[40]

Table 4. Kinetic Parameters for the Chemoselective Hydrogenation of Cinnamaldehyde over Au/SiO_2 and $Pt_{0.05}$^Au/SiO_2

catalyst	E_a[a]	A[b]	α[c]
Au/SiO_2	59.1	4.1	1.65
$Pt_{0.05}$^Au/SiO_2	55.1	40.0	1.29

[a] Apparent activation energy, kJ mol^{-1}. [b] Preexponential factor, mmol h^{-1} g_{cat}^{-1}. [c] Partial reaction order with respect to H_2.

On the other hand, the two catalysts responded quite differently to the reaction temperature with regard to product distribution. When the reaction temperature was elevated from 150 to 195 °C, the HCAL selectivity over Au/SiO_2 catalyst decreased from 73% to 55%, but the COL selectivity increased from 23% to 40%. In contrast, the product selectivity over $Pt_{0.05}$^Au/SiO_2 was kept essentially unchanged with the reaction temperature. The higher selectivity to COL over Au/SiO_2 catalyst at higher reaction temperature could be explained by a significantly higher barrier in C═O bond activation, since the dissociation energy of the C═O bond is 33 kcal mol^{-1} larger than that for the C═C bond.[14,41] Thus, the selectivity for C═O bond hydrogenation was enhanced with an increase in the reaction temperature over Au/SiO_2 catalyst. This reaction temperature effect on the product selectivity was not evident over $Pt_{0.05}$^Au/SiO_2; that is, the presence of Pt entities on Au NPs made the chemoselectivity insensitive to the reaction temperature.

H_2 dissociation is a very demanding surface reaction on Au that would occur only on edge and corner sites, but it becomes a facile reaction involving no activation barriers on a Pt surface.[26] We investigated the effect of hydrogen pressure on CAL hydrogenation over Au/SiO_2 and $Pt_{0.05}$^Au/SiO_2 catalyst to gain

dx.doi.org/10.1021/cs200247r |ACS Catal. 2011, 1, 1336–1346

Table 5. Langmuir−Hinshelwood Models for Cinnamaldehyde Hydrogenation over $Pt_{0.05}$^Au/SiO_2 Catalyst

rate-determining step	model[a]	linearized form[b]	R^{2c}
CAL adsorption	$r = \frac{k_{CAL} \cdot C_{CAL}}{1 + K_{H_2}^{1/2} \cdot P_{H_2}^{1/2}}$	$r^{-1} = a \cdot P_{H_2}^{1/2} + b$	0.791
H_2 dissociation	$r = \frac{k_{H_2} \cdot P_{H_2}}{(1 + K_{CAL} \cdot C_{CAL})^2}$	$r = a \cdot P_{H_2}$	0.956
surface reaction (competitive adsorption)	$r = \frac{k \cdot K_{CAL} \cdot K_{H_2} \cdot C_{CAL} \cdot P_{H_2}}{\left(1 + K_{CAL} \cdot C_{CAL} + K_{H_2}^{1/2} \cdot P_{H_2}^{1/2}\right)^3}$	$(P_{H_2}/r)^{1/3} = a \cdot P_{H_2}^{1/2} + b$	0.908
surface reaction (independent adsorption)	$r = \frac{k \cdot K_{CAL} \cdot K_{H_2} \cdot C_{CAL} \cdot P_{H_2}}{(1 + K_{CAL} \cdot C_{CAL}) \cdot \left(1 + K_{H_2}^{1/2} \cdot P_{H_2}^{1/2}\right)^2}$	$r^{-1/2} = a \cdot P_{H_2}^{-1/2} + b$	0.995

[a] k = rate constant for the surface reaction; k_{H_2} = rate constant for the H_2 dissociation; k_{CAL} = rate constant for the CAL adsorption; K_{H_2} = equilibrium constant for H_2 adsorption; K_{CAL} = equilibrium constant for CAL adsorption. [b] Because the change in C_{CAL} was insignificant (CAL conversion lower than 10%), a and b in the linearized forms are taken as constants. [c] Correlation coefficient obtained by linear regression.

information on the effect of Pt entities on the catalysis of Au in Pt_m^Au/SiO_2 samples. Table 3 lists the catalytic results as well as the global reaction rates by CAL consumption. Increasing P_{H_2} from 1.0 to 5.0 MPa for Au/SiO_2 and from 0.5 to 4.0 MPa for $Pt_{0.05}$^Au/SiO_2 resulted in continuous shortening of the reaction period for achieving a CAL conversion around 10%. When P_{H_2} was increased from 1.0 to 4.0 MPa, the reaction rate over Au/SiO_2 catalyst increased 11-fold. The same increase in H_2 pressure for the reaction over the $Pt_{0.05}$^Au/SiO_2 catalyst effected only a 5-fold increase in the reaction rate. Figure 6 presents the relationships between the reaction rate and P_{H_2} for both catalysts. The line slopes in this figure would give the partial reaction order with respect to H_2, which was 1.29 over $Pt_{0.05}$^Au/SiO_2 catalyst and 1.65 over Au/SiO_2 catalyst (Table 4).

For Au/SiO_2, the selectivity for HCAL decreased from 73% at P_{H_2} = 1.0 MPa to ∼50% at $P_{H_2} \geq$ 3.0 MPa, but at the same time, the selectivity for COL increased from 23% to around 40%. The hydrogen pressure effect on the selectivity of HCAL could be ascribed to a competitive adsorption of hydrogen with CAL on the Au sites.[21] For $Pt_{0.05}$^Au/SiO_2, however, the product distribution was little affected when the P_{H_2} was raised from 0.5 to 4.0 MPa (Table 3).

3.2.4. Kinetic modeling. Kinetic assessments of the CAL hydrogenation reaction on $Pt_{0.05}$^Au/SiO_2 were performed using catalytic data obtained at 150 °C under different P_{H_2} with the CAL conversion being limited to lower than 10% (Table 3). According to Langmuir−Hinshelwood kinetics, the following elementary steps, including reactant activation by adsorption of CAL (I) and H_2 (II), surface reaction between the adsorbed reactants (III) and desorption of product (IV), could be proposed as the key steps for the overall hydrogenation reaction:

$$\mathrm{CAL} + * \xrightarrow{k_{CAL}} \mathrm{CAL}* \quad \text{(I)}$$

$$\mathrm{H_2} + 2* \xrightarrow{k_{H_2}} 2\mathrm{H}* \quad \text{(II)}$$

$$\mathrm{CAL}* + 2\mathrm{H}* \xrightarrow{k} \mathrm{HCAL}* + 2* \quad \text{(III)}$$

$$\mathrm{HCAL}* \xrightarrow{k_{HCAL}} \mathrm{HCAL} + * \quad \text{(IV)}$$

HCAL was used as the representative product because it was the dominant compound in the products. Any product adsorption on the catalyst surface would be of no kinetic consequence, since the experiment kinetic rates were obtained with very high reactant/product ratios (the CAL conversion was <10%; Table 3) and the desorption of product (IV) would not be considered as a candidate for the rate-determining step.

Shown in Table 5 are the rate expressions when step I, II, and III were assumed, respectively, to be the rate-determining step. Note that only the rate-determining step could be taken as the irreversible step in deriving the rate expression. The two reactants (CAL and H_2) could adsorb with two possibilities: they could adsorb competitively on the same kind of surface sites or independently on two different kinds of surface sites. The two rate expressions for the surface reaction kinetics in Table 5 correspond to these two possibilities. Mathematical reformulation of the equations led to the linearized forms with respect to P_{H_2}. Linear regression using the experiment reaction rates under different P_{H_2} over the $Pt_{0.05}$^Au/SiO_2 catalyst (Table 3) produced the fitness results (R^2), which are given in the last column of Table 5. Apparently, the last kinetic model showed the highest fitness to the experiment data (R^2 = 0.995). Therefore, the rate-determining step of CAL hydrogenation over Pt_m^Au/SiO_2 catalysts would be the surface reaction between independently adsorbed CAL molecules and H atoms on active sites of different nature. These kinetic assessments identify that the active sites responsible for H_2 activation are different from those for CAL adsorption on Pt_m^Au/SiO_2.

4. DISCUSSION

This study corroborates our earlier observations[15] that a small amount of fully dispersed Pt deposits on Au NPs can lead to dramatic activity enhancement of the Au NPs for chemoselective hydrogenation of α,β-unsaturated compounds without changing the selectivity propensity of Au NPs. All of the catalytic reaction data presented in this work, including those acquired with varying reaction temperature and H_2 pressure, point to a synergic catalysis of Pt and Au in these Pt-on-Au (Pt_m^Au) nanostructures for the hydrogenation of CAL. It is further shown that the catalytic feature of Pt_m^Au was essentially not affected by the nature of their immobilizers or supporting materials.

To gain insight into the role of Pt in Pt_m^Au NPs for the hydrogenation catalysis, the reaction rates obtained on Pt_m^Au/SiO_2 catalysts were re-evaluated by normalizing the CAL consumption rate in Table 1 (CAL conversion, 11−20%) to the total

dx.doi.org/10.1021/cs200247r |ACS Catal. 2011, 1, 1336–1346

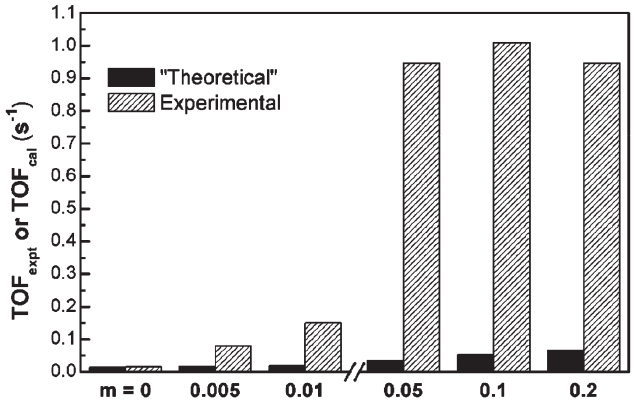

Figure 7. Experimental and "theoretical" TOF for cinnamaldehyde hydrogenation over Pt_m^Au/SiO_2 catalysts. The TOF numbers were calculated using eqs 1 and 2, respectively.

number of exposed metal (Pt + Au) atoms on Pt_m^Au NPs without discriminating Pt and Au atoms (TOF_{expt} as shown in eq 1). The total number of exposed metal atoms on Pt_m^Au NPs was estimated according to the size of Pt_m^Au NPs in the Pt_m^Au/SiO_2 samples, assuming that the NPs were cuboctahedrally structured.[42] For comparison, "theoretical" TOF numbers (TOF_{cal}) were also calculated by assuming an additive surface catalysis of exposed Au and Pt atoms (eq 2), in which the exposed Au and Pt atoms served independently as the catalytically active sites for the hydrogenation reaction. The TOF_{Au} and TOF_{Pt} in eq 2 were taken, respectively, as the experimental TOF numbers for the Au/SiO_2 and 1Pt/SiO_2−Sigma catalysts; the latter showed the highest TOF_{Pt} among the three Pt/SiO_2 catalysts (0.24 s^{-1}, Table 1). In addition, the X_{Pt} refers in eq 2 to Pt coverage on Au NPs, which was obtained with the assumption that every exposed Pt atom would bury one surface Au atom,[27,28] according to (eq 3).

$$TOF_{expt} = \frac{\text{reaction rate (mol/s)}}{\text{total number of exposed Au and Pt atoms (mol)}} \quad (1)$$

$$TOF_{cal} = TOF_{Au}(1 - X_{Pt}) + TOF_{Pt} \cdot X_{Pt} \quad (2)$$

$$X_{Pt} = \frac{\text{number of exposed Pt atoms (mol)}}{\text{total number of exposed Au and Pt atoms (mol)}} \quad (3)$$

Figure 7 shows the dependence of the experimental and theoretical TOF of Pt_m^Au/SiO_2 catalysts on the Pt loading (m). It is seen that TOF_{expt} for Pt_m^Au/SiO_2 increased steeply from 0.014 s^{-1} ($m = 0$) to around 1.0 s^{-1} when m increased up to $m = 0.05$ and then leveled off at $m \geq 0.1$. It is of interest to note that the TOF_{expt} number for every Pt_m^Au/SiO_2 catalyst at $m > 0.005$ was one magnitude higher than its corresponding TOF_{cal}. These results clearly demonstrate a synergy between Au NPs and their carrying Pt entities in Pt_m^Au nanostructures for the catalytic hydrogenation of CAL.

We showed in our preliminary communication that when benzyl alcohol was used instead of H_2 as the H-source for CAL hydrogenation (i.e., transfer hydrogenation reaction) over the same Pt_m^Au/SiO_2 catalysts, no synergic effect between Pt and Au could be observed.[15] Thus, the remarkable higher catalytic activity of Pt_m^Au/SiO_2 for CAL hydrogenation using

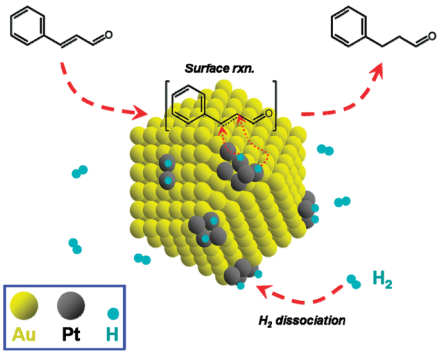

Figure 8. Synergy between Pt entities and their underlying Au NPs in the hydrogenation of cinnamaldehyde.

molecular H_2 would rely heavily on Pt promotion of H_2 activation. The present comparison of the H_2 pressure effect on the catalysis of Au/SiO_2 and $Pt_{0.05}$^Au/SiO_2 for CAL hydrogenation is in strong support of this catalytic chemistry. The partial reaction order with respect to H_2 decreased substantially from 1.65 for Au/SiO_2 to 1.29 for $Pt_{0.05}$^Au/SiO_2 (Table 4), which indicates that H_2 activation became less critical or much easier over the Pt_m^Au catalysts. Kinetic modeling of the hydrogenation reaction on Pt_m^Au/SiO_2 (Table 5) further indicates that H_2 and CAL would not compete for the same kind of adsorption sites: they adsorb respectively on two kinds of active sites with different properties in the Pt_m^Au nanostructures.

The activation energies and pre-exponential factors obtained from the Arrhenius plots for CAL hydrogenation over Au/SiO_2 and $Pt_{0.05}$^Au/SiO_2 catalysts (Table 4) indicate that the Pt enhancement of the Au activity was not due to a lowered energy barrier for the overall reaction, but the significantly increased pre-exponential factor (4.1 mmol h^{-1} g_{cat}^{-1} for Au/SiO_2 versus 40.0 mmol h^{-1} g_{cat}^{-1} for $Pt_{0.05}$^Au/SiO_2; Table 4). Because H_2 activation on Pt involves no activation barrier,[26] it appears reasonable that Pt entities on the Au NPs functioned as the new and more efficient catalytic sites for the H_2 activation and the uncovered Au sites were responsible for the adsorption/activation of the substrate CAL. The activated H atoms would then react with their nearby CAL molecules adsorbed on the Au surface, adopting the Langmuir−Hinshelwood mechanism (Table 5).

It is interesting to note that the synergy between Pt and Au in the hydrogenation catalysis over the Pt_m^Au nanostructures depended sensitively on the Pt dispersion (D_{Pt}) at the surface of Au NPs. The rate enhancement in either MSA_{Au} (Table 1) or TOF_{expt} (Figure 7) was proportional to Pt loading (m) for the Pt_m^Au/SiO_2 catalysts containing only fully dispersed Pt entities on the Au NPs ($m \leq 0.05$) but became almost insensitive to m for those catalysts containing less dispersed Pt entities ($m \geq 0.1$). Thus, the fully dispersed Pt entities showed the highest efficiency in enabling the synergic hydrogenation catalysis. This is not surprising, since for Au NPs carrying a fixed amount of Pt, the Pt−Au boundary would be maximized when the Pt was deposited as fully dispersed entities. However, the $Pt_{0.1}$^Au/SiO_2 catalyst of $D_{Pt} = 0.90$ would have much more Pt−Au boundary than a $Pt_{0.05}$^Au/SiO_2 of $D_{Pt} = 0.99$, but these two catalysts showed almost the same activity (Table 1). These comparisons suggest, therefore, that a proper proximity between Pt and Au sites would be required in the Pt_m^Au nanostructures to maximize the synergic catalysis. The lower TOF_{expt} (Figure 7) for the samples of $m = 0.005$ and 0.01 would be due to a significant percentage of Au sites

dx.doi.org/10.1021/cs200247r |ACS Catal. 2011, 1, 1336–1346

not being in the as-required proximity of Pt in these two samples. The lower efficiency of Pt in the samples of $m = 0.1$ and 0.2, on the other hand, could be due to some overpopulation of Pt entities at the surface of Au NPs, which also reduced the average number of Au sites in the as-required proximity of Pt.

The requirement for a proper proximity in maximizing the synergic catalysis could also explain why the bimetallic $Pt_{0.05}$−Au/SiO_2 catalyst showed a much lower activity than the $Pt_{0.05}$^Au/SiO_2 catalyst (Table 1). In comparison with $Pt_{0.05}$^Au/SiO_2, the bimetallic $Pt_{0.05}$−Au/SiO_2 catalyst could contain less dispersed Pt deposits, and a significant percentage of Pt could even be immobilized on the surface of SiO_2 and have no contact with Au NPs, since the preparation by impregnation of Au/SiO_2 with Pt cannot ensure a landing of Pt at the Au surface.

The Au NPs immobilized on the interacting Al_2O_3 and Vulcan XC-72 carbon showed significantly higher activity and lower selectivity for HCAL than the standard Au/SiO_2 catalyst for the hydrogenation reaction of CAL. In contrast, the $Pt_{0.05}$^Au immobilized on the three support materials (SiO_2, Al_2O_3, and Vulcan XC-72 carbon) showed similar activity and product selectivity in the reaction. These facts would demonstrate that the synergy between Au NPs and their carrying Pt well overweighed the effect of Au−support interaction on the hydrogenation catalysis (Table 1). Thus, the Pt entities in the immobilized $Pt_{0.05}$^Au catalysts dominated the activation of H_2 during the hydrogenation reaction, which is consistent with the conclusion from the kinetic assessments.

The product selectivity over Pt_m^Au/SiO_2 catalysts appeared also insensitive to the reaction temperature and H_2 pressure (Tables 2 and 3), which is again in strong contrast with the results obtained over the standard Au/SiO_2 catalyst. It has been known that the adsorption mode of α,β-unsaturated compounds is critical to their hydrogenation selectivity.[21,43,44] The insensitivity of product selectivity to the reaction temperature and H_2 pressure would hint that the presence of fully dispersed Pt entities on the surface of Au NPs could favor a specific adsorption mode for CAL activation. Further work is needed to uncover the details of CAL adsorption on Au and Pt_m^Au NPs.

5. CONCLUSIONS

Our data show that Pt in the nanostructured Pt_m^Au catalysts served as an efficient activity promoter to Au NPs in the hydrogenation of α,β-unsaturated compounds, by creating a new channel for H_2 activation. A synergy between Pt and Au was operating in the hydrogenation of CAL, in which Pt and Au sites functioned, respectively, for the activation of H_2 and CAL. The synergy depended critically on the dispersion of Pt entities and the Pt−Au proximity, but it was hardly affected by the temperature and H_2 pressure of the reaction. The overall reaction rate was determined by a Langmuir−Hinshelwood surface reaction step between independently adsorbed CAL and H atoms over the Pt_m^Au/SiO_2 catalysts. The well-maintained selectivity propensity for the hydrogenation reactions of Au catalyst in these novel Pt_m^Au nanostructures would have important implications for developing highly active nanogold catalysts, according to the metal-on-Au nanostructure models, for many selectivity-demanding hydrogenation reactions.

AUTHOR INFORMATION

Corresponding Author

*Phone/Fax: +86-10 6279 2122. E-mail: bqxu@mail.tsinghua.edu.cn.

ACKNOWLEDGMENT

This work was financially supported by the NSF of China (Grants 20921001, 21033004, and 21073103).

REFERENCES

(1) Carrettin, B.; McMorn, P.; Johnston, P.; Griffin, K.; Hutchings, G. J. *Chem. Commun.* **2002**, *7*, 696–697.
(2) Sun, K. Q.; Luo, S. W.; Xu, N.; Xu, B. Q. *Catal. Lett.* **2008**, *124*, 238–242.
(3) Turner, M.; Golovko, V. B.; Vaughan, O. P. H.; Abdulkin, P.; Berenguer-Murcia, A.; Tikhov, M. S.; Johnson, B. F. G.; Lambert, R. M. *Nature* **2008**, *454*, 981–984.
(4) Jia, J. F.; Haraki, K.; Kondo, J. N.; Domen, K.; Tamaru, K. *J. Phys. Chem. B* **2000**, *104*, 11153–11156.
(5) Zhang, X.; Shi, H.; Xu, B. Q. *Angew. Chem., Int. Ed.* **2005**, *44*, 7132–7135.
(6) Corma, A.; Serna, P. *Science* **2006**, *313*, 332–334.
(7) He, D. P.; Shi, H.; Wu, Y.; Xu, B. Q. *Green Chem.* **2007**, *9*, 849–851.
(8) Serna, P.; Concepcion, P.; Corma, A. *J. Catal.* **2009**, *265*, 19–25.
(9) Zhang, X.; Corma, A. *Angew. Chem., Int. Ed.* **2008**, *47*, 4358–4361.
(10) Corma, A.; Juarez, R.; Boronat, M.; Sanchez, F.; Iglesias, M.; Garcia, H. *Chem. Commun.* **2011**, *47*, 1446–1448.
(11) Grolig, J. *Ullmann's Encyclopedia of Industrial Chemistry*; Wiley-VCH: Weinheim, Germany, 2003.
(12) Milone, C.; Crisafulli, C.; Ingoglia, R.; Schipilliti, L.; Galvagno, S. *Catal. Today* **2007**, *122*, 341–351.
(13) Bus, E.; Prins, R.; van Bokhoven, J. A. *Catal. Commun.* **2007**, *8*, 1397–1402.
(14) Shi, H.; Xu, N.; Zhao, D.; Xu, B. Q. *Catal. Commun.* **2008**, *9*, 1949–1954.
(15) Hong, Y. C.; Sun, K. Q.; Zhang, G. R.; Zhong, R. Y.; Xu, B. Q. *Chem. Commun.* **2011**, *47*, 1300–1302.
(16) Claus, P.; Bruckner, A.; Mohr, C.; Hofmeister, H. *J. Am. Chem. Soc.* **2000**, *122*, 11430–11439.
(17) Mohr, C.; Hofmeister, H.; Claus, P. *J. Catal.* **2003**, *213*, 86–94.
(18) Okumura, M.; Nakamura, S.; Akita, T.; Haruta, M. *Catal. Today* **2002**, *74*, 265–269.
(19) Zanella, R.; Louis, C.; Giorgio, S.; Touroude, R. *J. Catal.* **2004**, *223*, 328–339.
(20) Claus, P. *Appl. Catal., A* **2005**, *291*, 222–229.
(21) Maki-Arvela, P.; Hajek, J.; Salmi, T.; Murzin, D.Yu. *Appl. Catal., A* **2005**, *292*, 1–49.
(22) Bus, E.; Miller, J. T.; van Bokhoven, J. A. *J. Phys. Chem. B* **2005**, *109*, 14581–14587.
(23) Bus, E.; van Bokhoven, J. A. *Phys. Chem. Chem. Phys.* **2007**, *9*, 2894–2902.
(24) Fujitani, T.; Nakamura, I.; Akita, T.; Okumura, M.; Haruta, M. *Angew. Chem., Int. Ed.* **2009**, *48*, 9515–9518.
(25) Buchanan, D. A.; Webb, G. *J. Chem. Soc. Faraday Trans.* **1975**, *71*, 134–144.
(26) Boronat, M.; Corma, A. *Langmuir* **2010**, *26*, 16607–16614.
(27) Zhao, D.; Xu, B. Q. *Angew. Chem., Int. Ed.* **2006**, *45*, 4955–4959.
(28) Zhao, D.; Xu, B. Q. *Phys. Chem. Chem. Phys.* **2006**, *8*, 5106–5114.
(29) Zhao, D.; Wang, Y. H.; Xu, B. Q. *J. Phys. Chem. C* **2009**, *113*, 20903–20911.
(30) Zhang, G. R.; Xu, B. Q. *Nanoscale* **2010**, *2*, 2798–2804.
(31) Li, W. Z.; Sun, K. Q.; Zhun, H.; Xu, B. Q. *Catal. Lett.* **2009**, *132*, 189–196.
(32) Miller, J. T.; Schreier, M.; Kropf, A. J.; Regalbuto, J. R. *J. Catal.* **2004**, *225*, 203–212.
(33) Xu, B. Q.; Wei, J. M.; Wang, H. Y.; Sun, K. Q.; Zhu, Q. M. *Catal. Today* **2001**, *68*, 217–221.
(34) Madon, R. J.; Boudart, M. *Ind. Eng. Chem. Fundam.* **1982**, *21*, 438–447.

(35) Muller, A.; Bowers, J. WO Patent 99/08989 (1999), to First Chemical Corporation.
(36) Oduro, W. O.; Cailuo, N.; Yu, K. M. K.; Yang, H. W.; Tsang, S. C. *Phys. Chem. Chem. Phys.* **2011**, *13*, 2590–2602; and references therein.
(37) Zhang, X.; Shi, H.; Xu, B. Q. *J. Catal.* **2011**, *279*, 75–87.
(38) Szollosi, G.; Torok, B.; Baranyl, L.; Bartok, M. *J. Catal.* **1998**, *179*, 619–623.
(39) Planeix, J. M.; Coustel, N.; Coq, B.; Brotons, V.; Kumbhar, P. S.; Dutartre, R.; Geneste, P.; Bernier, P.; Ajayan, P. M. *J. Am. Chem. Soc.* **1994**, *116*, 7935–7936.
(40) Zhang, L. Q.; Winterbottom, J. M.; Boyes, A. P.; Raymahasay, S. *J. Chem. Technol. Biotechnol.* **1998**, *72*, 264–272.
(41) Patil, A.; Banares, M. A.; Lei, X.; Fehlner, T. P.; Wolf, E. E. *J. Catal.* **1996**, *159*, 458–472.
(42) Lewis, L. N. *Chem. Rev.* **1993**, *93*, 2693–2730.
(43) Ponec, V. *Appl. Catal., A* **1997**, *149*, 27–48.
(44) Gallezot, P.; Richard, D. *Catal. Rev. — Sci. Eng.* **1998**, *40*, 81–126.